Stochastic modeling and generation of partially polarized or partially coherent electromagnetic waves

Brynmor Davis, Edward Kim, and J. R. Piepmeier

NASA Goddard Space Flight Center, Greenbelt, Maryland, USA

Received 24 July 2001; revised 7 January 2003; accepted 15 October 2003; published 15 January 2004.

[1] Many new Earth remote-sensing instruments are embracing both the advantages and added complexity that result from interferometric or fully polarimetric operation. To increase instrument understanding and functionality, a model of the signals these instruments measure is presented. A stochastic model is used as it recognizes the nondeterministic nature of any real-world measurements, while also providing a tractable mathematical framework. A wide-sense stationary, ergodic, Gaussian-distributed model structure is proposed. Temporal and spectral correlation measures provide a statistical description of the physical properties of coherence and polarization-state. From this relationship, the model is mathematically defined. A method of realizing the model (necessary for applications such as synthetic calibration-signal generation) is given, and computer simulation results are presented. The signals are constructed using the output of a multi-input, multi-output linear filter system, driven with white noise. *INDEX TERMS:* 6924 Radio Science: Interferometry; 6954 Radio Science: Radio astronomy; 6969 Radio Science: Remote sensing; 6974 Radio Science: Signal processing; *KEYWORDS:* interferometry, polarimetry, remote sensing

Citation: Davis, B., E. Kim, and J. R. Piepmeier (2004), Stochastic modeling and generation of partially polarized or partially coherent electromagnetic waves, *Radio Sci.*, *39,* RS1001, doi:10.1029/2001RS002512.

1. Introduction

[2] Radio-interferometers and polarimeters are being used more widely in remote sensing for probing the Earth's lands and oceans [e.g., *Swift et al.*, 1991; *Ruf*, 1988; *Yueh et al.*, 1997]. While these techniques have a rich history in the space sciences, Earth-viewing versions are relatively rare. For example, results from only two synthesis imaging radio-interferometer for airborne remote sensing appear in the literature. The Electronically-Scanned Thinned Array Radiometer (ESTAR) [*Le Vine et al.*, 2001; *Ruf and Principe*, 2003] uses interferometric imaging across-track and real aperture imaging along-track to image land and ocean surfaces from an aircraft. Recently, a Y-shaped 2-D synthesis imager was proposed for spaceflight [*Kerr*, 1998]. Earth Sensing using radio-polarimetry has a similar history, with several airborne instruments appearing in the last decade [*Yueh et al.*, 1995; *Piepmeier and Gasiewski*, 2001; *Bobak et al.*, 2001; *Lahtinen et al.*, 2001] and the launch of a spaceborne Earth-viewing polarimeter in 2003 [*Gaiser*, 1999].

[3] There are distinct differences in the operation and calibration techniques of ground-based space-viewing telescopes versus orbiting Earth-viewing instruments. Operationally, Earth-viewing imagers have a fraction of the integration time available compared to radio-telescopes: seconds versus hours. Additionally, radio-telescope elements have extremely narrow beams ($\sim 0.5^\circ$) compared to low-Earth orbit (LEO) synthesis imagers, whose wide beams ($\sim 60-90^\circ$) are required to image the entire Earth at least once per day. Perhaps more important are the calibration differences. Interferometric radio-telescopes are typically calibrated using extrasolar point sources, whereby the system can be characterized to within a common gain coefficient [*Thompson et al.*, 1991]. Furthermore, if the flux of the point source is known, the interferometer can be absolutely calibrated. There are no obvious point sources when looking downward at the Earth, at least ones that emit energy within the protected spectrum allocated for passive observing. Furthermore, because of their large beam widths, Earth-viewing interferometers cannot selectively view a single extrasolar point source. (Besides, the time and operations required for regularly rotating a spacecraft for calibration would cause data loss and increase mission risk.) Therefore, a different calibration technique must be devised for orbiting Earth-imaging systems. This paper lays the groundwork for such a technique by rigorously examining the signals that these radiometers measure.

0048-6604/04/2001RS002512$11.00

[4] While polarimetry and interferometry can be investigated independently, they are based upon a common concept—measuring the interdependence of two signals. For polarimetry these signals are the amplitudes of some orthogonal pair. In Earth remote sensing, vertical and horizontal polarizations are chosen because they correspond to the Earth's natural polarization basis as viewed from LEO. Two-beam interferometry involves measuring the coherence of two signals separated in space and/or time. In order to fully understand these instruments, it is desirable to have an accurate model of the types of signal pairs they measure. This type of model can be employed in mathematical analysis, computer simulations and for the generation of synthetic calibration signals (one possible on-orbit calibration tool).

[5] The developed model's structure and its applicability to useful physical problems is discussed in Section 2. Using this framework, Section 3 shows how a comprehensive model can be determined from the physical properties of the modeled wave(s). Section 4 gives a computational method for realizing the model. A polarimetric example is carried through Sections 2 and 3. This polarimetric example is implemented in Section 4 in order to demonstrate the ideas presented. A Summary is presented in the final section.

2. Model Structure and Applicability

2.1. Mathematical Model

[6] Electromagnetic waves generally have some degree of randomness—an unpolarized component in polarimetry or an incoherent component in interferometry. For this reason it is logical to employ a stochastic method when modeling the pair of signals. Using an analytic signal representation, the two signals of interest will be written as follows:

$$\begin{aligned} X(t) &= A(t)\cos\nu_0 t - B(t)\sin\nu_0 t \\ &= \mathrm{Re}\{[\mathrm{A(t)} + \mathrm{i\,B(t)}]\mathrm{e}^{\mathrm{i}\nu_0\mathrm{t}}\} \\ &= \mathrm{Re}\{\mathrm{P(t)}\mathrm{e}^{\mathrm{i}\nu_0\mathrm{t}}\} \\ Y(t) &= C(t)\cos\nu_0 t - D(t)\sin\nu_0 t \\ &= \mathrm{Re}\{[\mathrm{C(t)} + \mathrm{i\,D(t)}]\mathrm{e}^{\mathrm{i}\nu_0\mathrm{t}}\} \\ &= \mathrm{Re}\{\mathrm{Q(t)}e^{\mathrm{i}\nu_0\mathrm{t}}\} \end{aligned} \tag{1}$$

The functions are capitalized to indicate that they are random processes. Wide-sense stationarity is assumed so that the following temporal and spectral correlation functions can be defined.

$$\begin{aligned} E[\alpha(t)] &= \mu_\alpha \\ E[\alpha(t)\beta^*(t-\tau)] &= R_{\alpha\beta}(\tau) \\ S_{\alpha\beta}(\nu) &= \int_{-\infty}^{\infty} R_{\alpha\beta}(\tau)e^{i2\pi\nu\tau}d\tau \end{aligned} \tag{2}$$

where α and β can be X, Y, A, B, C, D, P or Q. Note that only $P(t)$ and $Q(t)$ are complex random processes, the rest are real.

2.2. Applying the Model

[7] This section shows how the mathematical model developed can be related to problems in interferometry and polarimetry. This is done by interpreting basic physical concepts in interferometry and polarimetry in terms of the mathematics of the model. It is left to the reader to explore relationships to specific systems [e.g., see *Christiansen and Högbom*, 1985].

2.2.1. Interferometry

[8] The model described above can be readily applied to two-beam interferometry through the mutual-coherence functions. This is done by assuming that the random processes used are ergodic. This allows the time averages present in the mutual-coherence functions (see *Born and Wolf* [1989] for a definition) to be equated to expected values. This idea is expressed below.

$$\begin{aligned} \Gamma_{11}(\tau) &= \langle P(t)P^*(t-\tau)\rangle = R_{PP}(\tau) \\ \Gamma_{22}(\tau) &= \langle Q(t)Q^*(t-\tau)\rangle = R_{QQ}(\tau) \\ \Gamma_{12}(\tau) &= \langle P(t)Q^*(t-\tau)\rangle = R_{PQ}(\tau) \end{aligned} \tag{3}$$

The equation above shows how basic coherence properties can be used to define the temporal correlation functions $R_{PP}(\tau)$, $R_{QQ}(\tau)$ and $R_{PQ}(\tau)$. In Section 3 it will be shown that these are sufficient to completely determine the second-order statistics of the model.

2.2.2. Polarimetry

[9] Stokes parameters are a tool commonly used to represent the polarization of an electromagnetic wave. Due to the fact that most conventional Earth imaging systems (e.g., the Special Sensor Microwave/Imager (SSM/I) spaceborne radiometer) measure the vertical and horizontal fields separately, the modified Stokes parameters [see *Ishimaru*, 1997], in brightness temperature, are typically used in Earth remote sensing. If the signal $X(t)$ from equation (1) is the horizontal field and $Y(t)$ is the vertical field, the following equation defines the modified Stokes parameters.

$$\begin{bmatrix} s_1 \\ s_2 \\ s_3 \\ s_4 \end{bmatrix} \propto \begin{bmatrix} \langle|P(t)|^2\rangle \\ \langle|Q(t)|^2\rangle \\ 2\mathrm{Re}\{\langle \mathrm{P(t)Q^*(t)}\rangle\} \\ 2\mathrm{Im}\{\langle \mathrm{P(t)Q^*(t)}\rangle\} \end{bmatrix} \tag{4}$$

The first two modified Stokes parameters are the power in the horizontal and vertical fields respectively—thus they are measured directly by most conventional Earth imaging systems.

[10] As shown in *Brosseau* [1998], the polarization states at different frequencies are uncorrelated. Thus, after invoking ergodicity, the modified Stokes parameters can be written as a function of frequency, which leads to the following result.

$$\begin{bmatrix} s_1(\nu) \\ s_2(\nu) \\ s_3(\nu) \\ s_4(\nu) \end{bmatrix} \propto \begin{bmatrix} S_{PP}(\nu) \\ S_{QQ}(\nu) \\ 2\mathrm{Re}\{S_{PQ}(\nu)\} \\ 2\mathrm{Im}\{S_{PQ}(\nu)\} \end{bmatrix} \tag{5}$$

So, for polarimetry, the modified Stokes parameters can be used to define the spectral correlation functions $S_{PP}(\nu)$, $S_{QQ}(\nu)$ and $S_{PQ}(\nu)$. An example of this follows. Note that the spectral correlation functions above are related to the temporal correlation functions $R_{PP}(\tau)$, $R_{QQ}(\tau)$ and $R_{PQ}(\tau)$ by a Fourier transform. This means Section 3 will also show that the spectral correlation functions are sufficient to completely determine the second-order statistics of the model.

[11] Example: The signal to be modeled has 5 distinct polarization bands within its overall bandwidth $2BW$. The lowest fifth of its spectrum is unpolarized and has unity power density ('modified Stokes densities' are [0.5, 0.5, 0, 0]); the second fifth has a degree of polarization of 0.5, unity power density and the polarized component is left-circular ([0.5, 0.5, 0, −0.5]); the central fifth is completely linearly polarized at 30° and has unity power density ([.75, .25, 0.866, 0]); the fourth section has a degree of polarization of 0.5, unity power density and the polarized component is right-circular ([0.5, 0.5, 0, 0.5]); and the highest frequency section is also unpolarized with unity power density ([0.5, 0.5, 0, 0]). By using equation (5), the model parameters shown in Table 1 are found.

[12] It can be shown that modified Stokes parameters for the total wave can be found by performing an integration over frequency. This results in the modified Stokes vector [1.1BW, 0.9BW, 0.346BW, 0].

3. Defining the Model

[13] Section 2.2 has shown how the mutual coherence functions (interferometric applications) or the modified Stokes parameters (polarimetric applications) can be used to define the second order statistics of the random process $P(t)$ and $Q(t)$. The task at hand is to show how these can in turn be used to completely determine the second-order statistics of the model.

3.1. Enforcing Stationarity

[14] The first step in this procedure is to enforce wide-sense stationarity on the signals to be measured ($X(t)$ and $Y(t)$.) Calculation of μ_X, μ_Y, $R_{XX}(\tau)$, $R_{YY}(\tau)$ and $R_{XY}(\tau)$ leads to the following conditions being needed for wide-sense stationarity.

Table 1. Spectral Functions Found From Example Polarization State

Frequency Band	$S_{PP}(\nu)$	$S_{QQ}(\nu)$	$S_{PQ}(\nu)$
$(-\infty, -BW]$	0	0	0
$(-BW, -0.6BW]$	0.5	0.5	0
$(-0.6BW, -0.2BW]$	0.5	0.5	$-0.25i$
$(-0.2BW, 0.2BW]$	0.75	0.25	0.433
$(0.2BW, 0.6BW]$	0.5	0.5	$0.25i$
$(0.6BW, BW]$	0.5	0.5	0
(BW, ∞)	0	0	0

$$\mu_A = \mu_B = \mu_C = \mu_D = 0 \tag{6}$$

$$\begin{gathered} R_{AA}(\tau) = R_{BB}(\tau) \\ R_{CC}(\tau) = R_{DD}(\tau) \\ R_{AC}(\tau) = R_{BD}(\tau) \\ R_{AD}(\tau) = -R_{BC}(\tau) \\ R_{AB}(\tau) = -R_{AB}(-\tau) \\ R_{CD}(\tau) = -R_{CD}(-\tau) \end{gathered} \tag{7}$$

The model's second-order statistics can be completely defined by the means and correlations of the constituent processes $A(t)$, $B(t)$, $C(t)$ and $D(t)$. The above equations are important because they show that rather than having four constants (the means) and ten functions (the correlations) to find, there are now only six unknown functions (two of which must be odd-symmetric.)

[15] Equation (6) implies $P(t)$ and $Q(t)$ are zero mean. The relations in equation (7) can be used to find the correlation functions of $P(t)$ and $Q(t)$.

$$\begin{aligned} R_{PP}(\tau) &= 2(R_{AA}(\tau) - iR_{AB}(\tau)) \\ R_{QQ}(\tau) &= 2(R_{CC}(\tau) - iR_{CD}(\tau)) \\ R_{PQ}(\tau) &= 2(R_{AC}(\tau) - iR_{AD}(\tau)) \end{aligned} \tag{8}$$

The equations above are significant because there is now only one real function defining each of the real and imaginary parts of the spectra of $P(t)$ and $Q(t)$.

[16] An interesting result can be stated from equation (7). By looking at a single signal (say $X(t)$) and its in-phase and quadrature components ($A(t)$ and $B(t)$) it can be seen

that $R_{AA}(0) = R_{BB}(0)$ and $R_{AB}(0) = 0$. This means that at any given time the in-phase and quadrature components have the same variance and are uncorrelated. For a Gaussian process, the result is that the amplitude of the signal is Rayleigh distributed and the phase is uniformly distributed. This result is stated in *Brosseau* [1998].

3.2. Mathematical Model Definition

[17] Equations (7) and (8) imply that there is only one set of correlation functions for $A(t)$, $B(t)$, $C(t)$ and $D(t)$ that will produce a given set of correlation functions for $P(t)$ and $Q(t)$. This set of correlation functions can be found (in both the temporal and spectral domains) easily from equation (8) by the method shown below. It should be noted that equation (7)'s odd-symmetry condition on $R_{AB}(\tau)$ and $R_{CD}(\tau)$ is always satisfied due to the conjugate symmetry of $R_{PP}(\tau)$ and $R_{QQ}(\tau)$.

$$
\begin{aligned}
R_{AA}(\tau) &= \frac{1}{2}\mathrm{Re}\{\mathrm{R_{PP}}(\tau)\} = \frac{1}{4}\left\{\mathrm{R_{PP}}(\tau) + \mathrm{R^{*}_{PP}}(\tau)\right\} \\
\Rightarrow S_{AA}(\nu) &= \frac{1}{4}\left[S_{PP}(\nu) + S_{PP}(-\nu)\right] \\
R_{CC}(\tau) &= \frac{1}{2}\mathrm{Re}\left\{\mathrm{R_{QQ}}(\tau)\right\} = \frac{1}{4}\left\{\mathrm{R_{QQ}}(\tau) + \mathrm{R^{*}_{QQ}}(\tau)\right\} \\
\Rightarrow S_{CC}(\nu) &= \frac{1}{4}\left[S_{QQ}(\nu) + S_{QQ}(-\nu)\right] \\
R_{AB}(\tau) &= \frac{-1}{2}\mathrm{Im}\{\mathrm{R_{PP}}(\tau)\} = \frac{\mathrm{i}}{4}\left\{\mathrm{R_{PP}}(\tau) - \mathrm{R^{*}_{PP}}(\tau)\right\} \\
\Rightarrow S_{AB}(\nu) &= \frac{i}{4}\left[S_{PP}(\nu) - S_{PP}(-\nu)\right] \\
R_{CD}(\tau) &= \frac{-1}{2}\mathrm{Im}\left\{\mathrm{R_{QQ}}(\tau)\right\} = \frac{\mathrm{i}}{4}\left\{\mathrm{R_{QQ}}(\tau) - \mathrm{R^{*}_{QQ}}(\tau)\right\} \\
\Rightarrow S_{CD}(\nu) &= \frac{i}{4}\left[S_{QQ}(\nu) - S_{QQ}(-\nu)\right] \\
R_{AC}(\tau) &= \frac{1}{2}\mathrm{Re}\left\{\mathrm{R_{PQ}}(\tau)\right\} = \frac{1}{4}\left\{\mathrm{R_{PQ}}(\tau) + \mathrm{R^{*}_{PQ}}(\tau)\right\} \\
\Rightarrow S_{AC}(\nu) &= \frac{1}{4}\left[S_{PQ}(\nu) + S^{*}_{PQ}(-\nu)\right] \\
R_{AD}(\tau) &= \frac{-1}{2}\mathrm{Im}\left\{\mathrm{R_{PQ}}(\tau)\right\} = \frac{\mathrm{i}}{4}\left\{\mathrm{R_{PQ}}(\tau) - \mathrm{R^{*}_{PQ}}(\tau)\right\} \\
\Rightarrow S_{AD}(\nu) &= \frac{i}{4}\left[S_{PQ}(\nu) - S^{*}_{PQ}(-\nu)\right] \qquad (9)
\end{aligned}
$$

By using the equations above and the first four equalities in equation (7), all the correlation functions of $A(t)$, $B(t)$, $C(t)$ and $D(t)$ can be found. This leads to a model that has completely specified second-order statistics; and that specification is unique (i.e., it is the only one that will produce the desired correlation functions for $P(t)$ and $Q(t)$ while maintaining stationarity of $X(t)$ and $Y(t)$).

Table 2. Model Spectral Functions Found for Example in Section 2.2.2

Frequency Band	$S_{AA}(\nu) = S_{BB}(\nu)$	$S_{CC}(\nu) = S_{DD}(\nu)$	$S_{AB}(\nu)$	$S_{CD}(\nu)$	$S_{AC}(\nu) = S_{BD}(\nu)$	$S_{AD}(\nu) = -S_{BC}(\nu)$
$(-\infty, -BW]$	0	0	0	0	0	0
$(-BW, -0.6BW]$	0.25	0.25	0	0	0	0
$(-0.6BW, -0.2BW]$	0.25	0.25	0	0	0	−0.125
$(-0.2BW, 0.2BW]$	0.375	0.125	0	0	0.217	0
$(0.2BW, 0.6BW]$	0.25	0.25	0	0	0	0.125
$(0.6BW, BW]$	0.25	0.25	0	0	0	0
(BW, ∞)	0	0	0	0	0	0

[18] Example: This process was applied to the spectral functions from the example in Section 2.2.2. Using equation (9), the results are shown in Table 2.

3.3. Summary of Model Design

[19] A brief summary of the model design follows:

[20] 1. Define the spectral or correlation functions of $P(t)$ and $Q(t)$ by considering the physical properties (either interferometric or polarimetric) of the waves to be modeled.

[21] 2. Apply equation (9) to get six valid spectral or correlation functions for $A(t)$, $B(t)$, $C(t)$ and $D(t)$.

[22] 3. Apply equation (7) to get the complete set of second-order statistical functions of the random processes $A(t)$, $B(t)$, $C(t)$ and $D(t)$ and thus completely define the model (up to second-order statistics.)

[23] It should be noted that there is no loss of generality in any of the steps, and that a single set of physical parameters can only produce one valid model (up to second-order statistics.)

4. Realizing the Model

[24] The previous sections have developed a stochastic model for a pair of signals. This model is defined by the temporal and spectral correlation functions of $A(t)$, $B(t)$, $C(t)$ and $D(t)$. These are found from physical signal properties. This is a clear mathematical model that has the potential to be useful in theoretical analysis. However, for applications such as computer simulations and synthetic signal generation it is necessary to create realizations of these random processes. It is sufficient to create realizations of the real variables $A(t)$, $B(t)$, $C(t)$ and $D(t)$, as the other variables ($P(t)$, $Q(t)$, $X(t)$ and $Y(t)$) can be created by deterministic functions of these four realizations. To do this an assumption about the probability distribution of the processes will need to be made. The obvious choice is to assume a Gaussian distribution. This can be justified by appealing to the Central Limit Theorem and has the advantage that it can be defined by the second-order statistics the model gives. This results in the required wide-sense stationary, ergodic process.

[25] Once the probability density functions are known, it is possible to create a sampled realization directly. If N points of data were required, the correlation matrix for these points could be calculated and a multivariate, Gaussian random number generator applied (such as the mvnrnd command found in the MATLAB software package.) However, difficulties arise when the dimensionality of this p.d.f. is considered. There are four codependent outputs at every sample so a signal of length N would have a p.d.f. of dimension $4N$. For example, a signal of 125 MHz bandwidth requires a minimum sampling rate of 250×10^6 samples per second—thus a two-second signal would require 500×10^6 samples and result in a probability density function of dimension two billion. This is computationally impractical so a simpler method must be found.

[26] A common technique in one dimension is to use a linear filter to shape noise into a desired spectral shape. The problem here is more complicated as the function is from one dimension (time) into four dimensions ($A(t)$, $B(t)$, $C(t)$, $D(t)$). A generalized filter structure with N inputs ($I_1(t)$, $I_2(t)$, …, $I_N(t)$) and M outputs ($O_1(t)$, $O_2(t)$, …, $O_M(t)$) is given below (this structure is presented in *Jenkins and Watts* [1968]).

$$\begin{aligned} O_1(t) &= \sum_{i=1}^{N} h_{1i}(t) * I_i(t) \\ O_2(t) &= \sum_{i=1}^{N} h_{2i}(t) * I_i(t) \\ &\vdots \\ O_M(t) &= \sum_{i=1}^{N} h_{Mi}(t) * I_i(t) \end{aligned} \tag{10}$$

The filter responses must be chosen so that the desired correlation functions are realized. These functions are given by the expressions below [*Jenkins and Watts*, 1968].

$$\begin{aligned} R_{O_pO_q}(\tau) &= E\left[O_p(t)O_q(t-\tau)\right] \quad \left(= R_{O_qO_p}(-\tau)\right) \\ &= E\left[\left(\sum_{i=1}^{N} h_{pi}(t) * I_i(t)\right)\right. \\ &\quad \left.\cdot\left(\sum_{j=1}^{N} h_{qj}(t-\tau) * I_j(t-\tau)\right)\right] \\ &= E\left[\sum_{i=1}^{N}\sum_{j=1}^{N}\left(h_{pi}(t) * I_i(t)\right)\right. \\ &\quad \left.\cdot\left(h_{qj}(t-\tau) * I_j(t-\tau)\right)\right] \\ &= \sum_{i=1}^{N}\sum_{j=1}^{N} R_{I_iI_j}(\tau) * h_{pi}(\tau) * h_{qj}(-\tau) \end{aligned} \tag{11}$$

This set of equations has a simpler form in the Fourier domain, as the convolutions become multiplications.

$$\begin{aligned} S_{O_pO_q}(\nu) &= \sum_{i=1}^{N}\sum_{j=1}^{N} S_{I_iI_j}(\nu) H_{pi}(\nu) H_{qj}(-\nu) \\ &= \sum_{i=1}^{N}\sum_{j=1}^{N} S_{I_iI_j}(\nu) H_{pi}(\nu) H_{qj}^{*}(\nu) \end{aligned} \tag{12}$$

The final step takes advantage of conjugate symmetry (which is guaranteed by the fact that $h_{mn}(t)$ is real for all mn.)

[27] A general set of solutions for the system of equations given by equation (12) is nontrivial as the system is nonlinear. Simplifications can be made by making certain assumptions—the first of which is that the input random processes are independent, white, Gaussian, unit variance and zero mean (so $S_{X_iX_j}(\nu) = \delta(i-j)$.) This ensures the outputs will be Gaussian and zero mean as required; and that equation (12) reduces to the form given below.

$$\begin{aligned} S_{O_pO_q}(\nu) &= \sum_{i=1}^{N}\sum_{j=1}^{N} \delta(i-j) H_{pi}(\nu) H_{qj}^{*}(\nu) \\ &= \sum_{i=1}^{N} H_{pi}(\nu) H_{qi}^{*}(\nu) \end{aligned} \tag{13}$$

In this case only four output processes are required ($M = 4$.) This means we have ten independent equations—one for each of the correlation functions given in equation (7) (there are 16 equations but there is redundancy, as shown by the bracketed term in equation (11)). A solution is presented for the case of four input processes (i.e., $N = 4$) although the method can be applied to larger dimensions provided that $M = N$ and the specified spectra satisfy the properties of a spectral matrix. The equations for this problem (as defined by equation (13)) are given below (the ν dependence has been dropped for clarity.) The outputs are denoted by A, B, C, D as before, while the inputs are numbered 1, 2, 3, 4.

$$\begin{aligned} S_{AA} &= |H_{A1}|^2 + |H_{A2}|^2 + |H_{A3}|^2 + |H_{A4}|^2 \\ S_{AB} &= H_{A1}H_{B1}^{*} + H_{A2}H_{B2}^{*} + H_{A3}H_{B3}^{*} + H_{A4}H_{B4}^{*} \\ S_{AC} &= H_{A1}H_{C1}^{*} + H_{A2}H_{C2}^{*} + H_{A3}H_{C3}^{*} + H_{A4}H_{C4}^{*} \\ S_{AD} &= H_{A1}H_{D1}^{*} + H_{A2}H_{D2}^{*} + H_{A3}H_{D3}^{*} + H_{A4}H_{D4}^{*} \\ S_{BB} &= |H_{B1}|^2 + |H_{B2}|^2 + |H_{B3}|^2 + |H_{B4}|^2 \\ S_{BC} &= H_{B1}H_{C1}^{*} + H_{B2}H_{C2}^{*} + H_{B3}H_{C3}^{*} + H_{B4}H_{C4}^{*} \\ S_{BD} &= H_{B1}H_{D1}^{*} + H_{B2}H_{D2}^{*} + H_{B3}H_{D3}^{*} + H_{B4}H_{D4}^{*} \\ S_{CC} &= |H_{C1}|^2 + |H_{C2}|^2 + |H_{C3}|^2 + |H_{C4}|^2 \\ S_{CD} &= H_{C1}H_{D1}^{*} + H_{C2}H_{D2}^{*} + H_{C3}H_{D3}^{*} + H_{C4}H_{D4}^{*} \\ S_{DD} &= |H_{D1}|^2 + |H_{D2}|^2 + |H_{D3}|^2 + |H_{D4}|^2 \end{aligned} \tag{14}$$

Although these equations are nonlinear, they can still be solved relatively easily. The solution method developed is most succinctly expressed in matrix notation.

$$\overline{\overline{H}} = \begin{bmatrix} H_{A1} & H_{A2} & H_{A3} & H_{A4} \\ H_{B1} & H_{B2} & H_{B3} & H_{B4} \\ H_{C1} & H_{C2} & H_{C3} & H_{C4} \\ H_{D1} & H_{D2} & H_{D3} & H_{D4} \end{bmatrix} \tag{15}$$

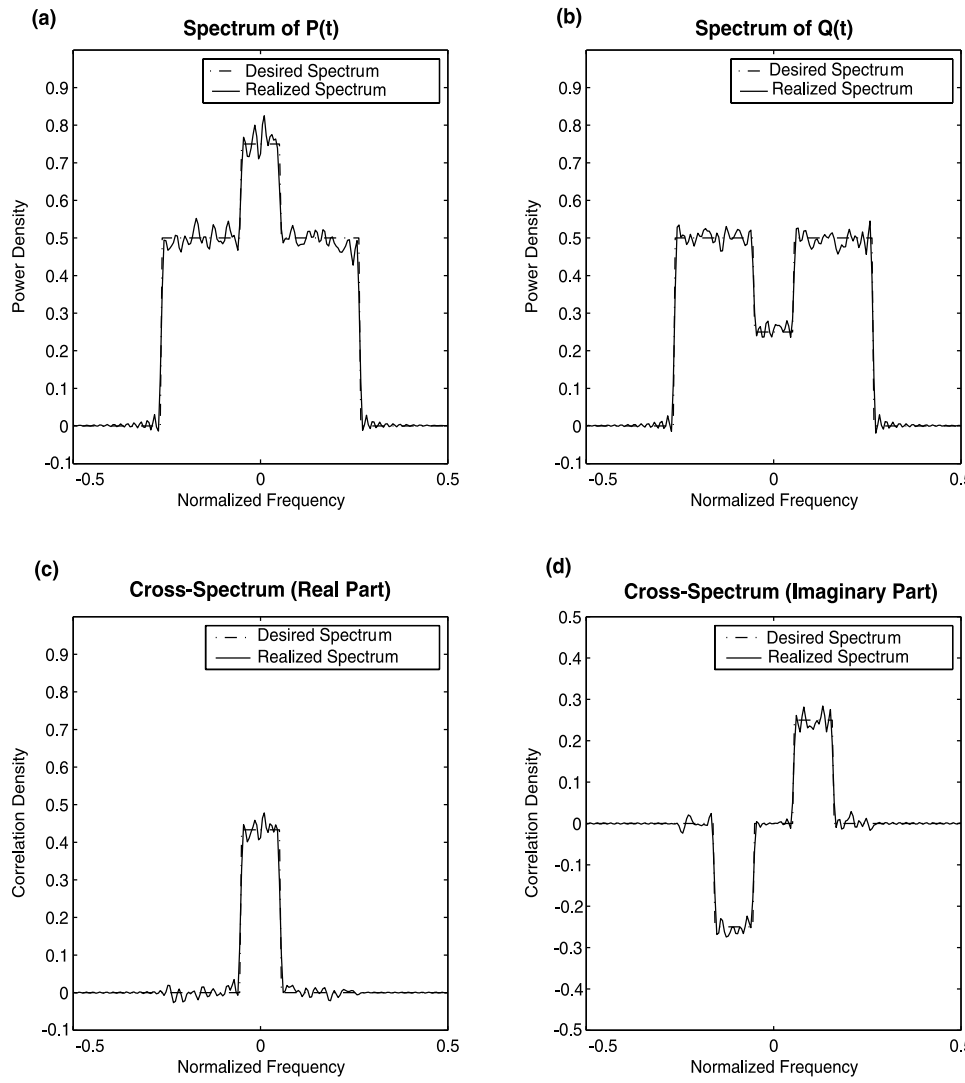

Figure 1. Resulting spectra for the example of Section 2.2.2.

$$\overline{\overline{S}} = \begin{bmatrix} S_{AA} & S_{AB} & S_{AC} & S_{AD} \\ S_{AB}^* & S_{BB} & S_{BC} & S_{BD} \\ S_{AC}^* & S_{BC}^* & S_{CC} & S_{CD} \\ S_{AD}^* & S_{BD}^* & S_{CD}^* & S_{DD} \end{bmatrix} \tag{16}$$

Using this notation, equation (14) can be rewritten as shown below.

$$\overline{\overline{S}} = \overline{\overline{H}}\,\overline{\overline{H}}^{\dagger} \tag{17}$$

For matrices the † operation represents a conjugate transpose. In order to find a suitable set of filters it is sufficient to solve equation (17) at the frequency points of interest. It is shown in *Strang* [1976] that because $\overline{\overline{S}}$ is positive semidefinite (always the case for spectral matrices such as this [*Jenkins and Watts*, 1968]), equation (17) can always be solved. A method for doing this is outlined below.

[28] Because the spectral matrix $\overline{\overline{S}}$ is Hermitian, it is always unitarily diagonalizable, its eigenvalues are real and its eigenvectors are orthogonal. This allows a simple solution for equation (17) to be found by using the diagonalized form of $\overline{\overline{S}}$. If the eigenvalues are arranged on the main diagonal in the matrix $\overline{\Lambda}$ and

the eigenvectors in the matrix $\overline{\overline{E}}$ then the following is true.

$$\begin{aligned}\overline{\overline{S}} &= \overline{\overline{E}}\,\overline{\overline{\Lambda}}\,\overline{\overline{E}}^{\dagger}\\ \overline{\overline{S}} &= \overline{\overline{E}}\sqrt{\overline{\overline{\Lambda}}}\sqrt{\overline{\overline{\Lambda}}}\,\overline{\overline{E}}^{\dagger}\\ \overline{\overline{S}} &= \left(\overline{\overline{E}}\sqrt{\overline{\overline{\Lambda}}}\right)\left(\overline{\overline{E}}\sqrt{\overline{\overline{\Lambda}}}^{\dagger}\right)^{\dagger}\\ \overline{\overline{S}} &= \left(\overline{\overline{E}}\sqrt{\overline{\overline{\Lambda}}}\right)\left(\overline{\overline{E}}\sqrt{\overline{\overline{\Lambda}}}\right)^{\dagger}\end{aligned} \tag{18}$$

$\sqrt{\overline{\overline{\Lambda}}}$ is a matrix with the square-roots of the eigenvalues on the main diagonal (so that $\sqrt{\overline{\overline{\Lambda}}}\sqrt{\overline{\overline{\Lambda}}} = \overline{\overline{\Lambda}}$.) Positive semidefiniteness guarantees the eigenvectors are nonnegative, so $\sqrt{\overline{\overline{\Lambda}}}$ will always be a real matrix and hence be equal to its own conjugate transpose.

[29] By comparing equation (18) with equation (17) it can be seen that the filter responses can be calculated by as follows:

$$\overline{\overline{H}} = \overline{\overline{E}}\sqrt{\overline{\overline{\Lambda}}} \tag{19}$$

Equation (19) shows how equation (14) can be solved by finding the eigenvalues and eigenvectors of the spectral matrix $\overline{\overline{S}}$ at each frequency point. It is easy to show that this method will produce filter spectra that are conjugate-symmetric, which is necessary to ensure that the filters have a real response. Reordering the eigenvalues and eigenvectors will still result in a valid solution at a single frequency point but care should be taken not to do this when constructing functions over many frequency points. Doing so would result in a sharp discontinuity in the filter spectra produced which would increase the length of the filter impulse response.

[30] In this section it has been shown how independent, white, Gaussian noise functions (which are easily generated) can be fed into a system of linear filters to produce realizations of the model. The filter sets are generated using equation (19) which depends on the model parameters. This process is computationally tractable and produces results like those shown in the example below.

[31] Example: The example functions coming from the signal in section 2.2.2 were realized using the methodology given in this section. This process was carried out using MATLAB and plots of the resulting spectra can be seen in Figure 1. It can be seen that the frequency axes extend outside the region $[-BW, BW]$—this corresponds to oversampling. The frequency axes are normalized so that the range of unaliased frequencies falls between -0.5 and 0.5.

[32] The estimates of the realized spectra were found using periodogram averaging. Four hundred spectra were averaged in each case, and a rectangular window was used in the time domain to remove the noisy terms associated with a large $|\tau|$. Each plot has 399 frequency points and the filters were truncated to 199 taps. Figure 1 shows that the resulting spectra agree closely with those specified. The small differences can be accounted for by the necessary truncation of the generation filters and by the fact that a finite number of spectra were used to create the periodogram average. The above model realization can be readily translated into space-qualifiable microwave circuitry for use in the characterization Earth-imaging correlation radiometers (a subject for a separate paper).

5. Summary

[33] This paper begins by showing how standard measures in polarimetry and interferometry (such as Stokes parameters and mutual-coherence functions) can be interpreted in terms of the model's temporal or spectral correlation functions. This statistical interpretation then allows a stationary, Gaussian model of the signal pair to be defined. A stationary, Gaussian model can be justified physically in Earth remote sensing as the sources are natural thermal radiation. Additionally, the stationarity assumption was shown to lead to a unique model for any given set of physical properties. This indicates a comprehensive, well defined stochastic model in either the polarimetric or interferometric paradigm.

[34] To realize this signal (as would be required in such applications as synthetic calibration-signal generation), it is necessary to produce a signal pair that has the same properties as the model. This can be done by generalizing a well-known noise-shaping technique in which a white, Gaussian process is passed through a linear filter in order to color its spectrum to a desired shape. The method was corroborated by presenting results from a MATLAB implementation.

References

Bobak, J., D. Dowgiallo, N. McGlothlin, and K. S. Germain (2001), APMIR: Airborne Polarimetric Microwave Imaging Radiometer, in *Proceedings of International Geoscience and Remote Sensing Symposium*, vol. 1, pp. 505–507, IEEE Press, Piscataway, N. J.

Born, M., and E. Wolf (1989), *Principles of Optics*, 6th ed., chap. 10, p. 500, Pergammon, New York.

Brosseau, C. (1998), *Fundamentals of Polarized Light*: *A Statistical Optics Approach*, chap. 3, John Wiley, Hoboken, N. J.

Christiansen, W. N., and J. A. Högbom (1985), *Radiotelescopes*, Cambridge Univ. Press, New York.

Gaiser, P. W. (1999), WindSat satellite-based polarimetric microwave radiometer, paper presented at International Microwave

Symposium, Inst. of Electr. and Electron. Eng., Anaheim, Calif.

Ishimaru, A. (1997), *Wave Propagation and Scattering in Random Media*, chap. 2, pp. 31–32, Oxford Univ. Press, New York.

Jenkins, G. W., and D. G. Watts (1968), *Spectral Analysis and Its Applications*, chap. 8, p. 11, Holden-Day, Boca Raton, Fla.

Kerr, Y. H. (1998), SMOS: Proposal in answer to the [European Space Agency's] call for Earth Explorer Opportunity Missions COP-16, Cent. d'Etudes Spatiales de la Biosphre, Toulouse, France.

Lahtinen, J., S. Tauriainen, and M. Hallikainen (2001), HUT fully polarimetric radiometer system, in *Proceedings of International Geoscience and Remote Sensing Symposium*, vol. 1, pp. 360–362, IEEE Press, Piscataway, N. J.

Le Vine, D., T. Jackson, C. Swift, M. Haken, and S. Bidwell (2001), ESTAR measurements during the Southern Great Plains Experiment (SGP99), *IEEE Trans. Geosci. Remote Sens.*, *39*(8), 1680–1685.

Piepmeier, J. R., and A. J. Gasiewski (2001), High-resolution passive microwave polarimetric mapping of ocean surface wind vector fields, *IEEE Trans. Geosci. Remote Sens.*, *39*(3), 606–622.

Ruf, C. (1988), Interferometric synthetic aperture microwave radiometry for the remote sensing of the Earth, *IEEE Trans. Geosci. Remote Sens.*, *26*(5), 597–611.

Ruf, C., and C. Principe (2003), X-band lightweight rainfall radiometer first light, in *Proceedings of International Geoscience and Remote Sensing Symposium*, vol. 3, pp. 1701–1703, IEEE Press, Piscataway, N. J.

Strang, G. (1976), *Linear Algebra and Its Applications*, chap. 6, Academic, San Diego, Calif.

Swift, C. T., D. M. LeVine, and C. S. Ruf (1991), Aperture synthesis concepts in microwave remote sensing of the Earth, *IEEE Trans. Microwave Theory Tech.*, *39*, 1931–1935.

Thompson, A. R., J. M. Moran, and G. W. Swenson Jr. (1991), *Interferometry and Synthesis in Radio Astronomy*, Krieger, Melbourne, Fla.

Yueh, S., W. Wilson, F. Li, S. Nghiem, and W. Ricketts (1995), Polarimetric measurements of sea surface brightness temperatures using an aircraft K-band radiometer, *IEEE Trans. Geosci. Remote Sens.*, *33*, 85–92.

Yueh, S., W. Wilson, F. Li, W. Ricketts, and S. Nghiem (1997), Polarimetric brightness temperature of sea surfaces measured with K- and Ka-band radiometers, *IEEE Trans. Geosci. Remote Sens.*, *35*, 1177–1187.

B. Davis, E. Kim, and J. R. Piepmeier, NASA Goddard Space Flight Center, Greenbelt, MD 20771, USA. (Ed.Kim@nasa.gov)